

Contents lists available at ScienceDirect

Journal of Advanced Research

journal homepage: www.elsevier.com/locate/jare



Piezo1 activation accelerates osteoarthritis progression and the targeted therapy effect of artemisinin



Donghao Gan^{a,1}, Chu Tao^{a,1}, Xiaowan Jin^{a,1}, Xiaohao Wu^{a,1}, Qinnan Yan^a, Yiming Zhong^a, Qingyun Jia^b, Lisheng Wu^b, Shaochuan Huo^c, Lei Qin^d, Guozhi Xiao^{a,*}

- ^a Department of Biochemistry, School of Medicine, Guangdong Provincial Key Laboratory of Cell Microenvironment and Disease Research, Shenzhen Key Laboratory of Cell Microenvironment. Southern University of Science and Technology, Shenzhen, China
- ^b Department of Orthopedics, Linyi People's Hospital, Linyi, China
- ^c Shenzhen Hospital (Futian) of Guangzhou University of Chinese Medicine, Shenzhen, China
- ^d Department of Orthopedics, Huazhong University of Science and Technology Union Shenzhen Hospital, Shenzhen, China

HIGHLIGHTS

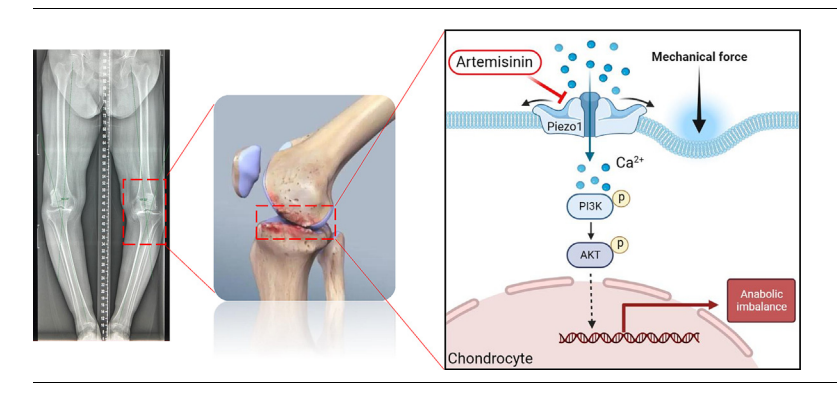
- Using genetic mouse models and a synthetic small molecule activator to demonstrate that Piezo1 activation promotes OA development and progression.
- Utilizing biochemical and histological approaches to reveal that Piezo1 activation promotes Runx2 expression and chondrocyte catabolism through a PI3K-AKT dependent manner.
- Demonstrated that artemisinin protects against OA lesions by inactivating Piezo1 in mice.

ARTICLE INFO

Article history:
Received 14 May 2023
Revised 23 September 2023
Accepted 24 September 2023
Available online 25 September 2023

Keywords: Osteoarthritis Piezo1 Artemisinin Chondrocyte

G R A P H I C A L A B S T R A C T



ABSTRACT

Introduction: Osteoarthritis (OA) is a devastating whole-joint disease affecting a large population worldwide with no cure; its mechanism remains poorly defined. Abnormal mechanical stress is the main pathological factor of OA.

Objectives: To investigate the effects of Piezo1 activation on OA development and progression and to explore Piezo1-targeting OA treatment.

Methods: The expression levels of Piezo1 were determined in human OA cartilage and experimental OA mice. Mice with genetic Piezo1 deletion in chondrocytes or intra-articular injection of the Piezo1 activator Yoda1 were utilized to determine the effects on DMM-induced OA progression. Effects of artemisinin (ART), a potent antimalarial drug, on Piezo1 activation, chondrocyte metabolism and OA lesions were determined.

Results: Piezo1 expression was elevated in articular chondrocytes in human OA and DMM-induced mouse OA cartilage. Piezo1 deletion in chondrocytes largely attenuates DMM-induced OA-like phenotypes. In contrast, intra-articular injection of Yoda1 aggravates the knee joint OA lesions in mice. PIEZO1 activation increases, while PIEZO1 siRNA knockdown decreases, expression of RUNX2 and catabolic enzymes MMP13 and ADAMTS5 in primary human articular chondrocytes in a PI3K-AKT dependent manner. We have provided strong evidence supporting that ART is a novel and potent inhibitor of Piezo1

E-mail address: xiaogz@sustech.edu.cn (G. Xiao).

^{*} Corresponding author.

¹ These authors contributed equally.

activation in primary OA-HACs and all cell lines examined, including human endothelial HUVEC cells, ATDC5 chondrocyte-like cells and MLO-Y4 osteocytes-like cells. Results from in vitro experiments confirmed that ART decreases the Yoda1-induced increases in the levels of OA-related genes and p-PI3K and p-AKT proteins in OA-HACs and alleviates DMM-induced OA lesions in mice.

Conclusions: We establish a critical role of Piezo1 in promoting OA development and progression and define ART as a potential OA treatment.

© 2024 The Authors. Published by Elsevier B.V. on behalf of Cairo University. This is an open access article under the CC BY-NC-ND license (http://creativecommons.org/licenses/by-nc-nd/4.0/).

Introduction

Osteoarthritis (OA) is a chronic whole-joint disease that involves the articular cartilage, synovium and subchondral bone. Articular cartilage degeneration is the main pathological feature of OA [1]. Epidemiological studies have shown that globally, the prevalence of OA has increased from 4.71 % in 1990 to 6.85 % in 2019, with a 113.25 % increase in the number of patients. The prevalence of OA in China has increased from 4.53 % in 1990 to 6.94 % in 2019, and the number of patients has significantly increased by 156.58 %. In terms of prevalence, the incidence of OA in China has risen rapidly in the past 30 years [2]. It is estimated that larger than 300 million people worldwide suffer from OA, which costs about 300 billion US dollars in medical expenses and income loss every year [3]. With the aggravation of population aging and obesity, the incidence and disability rate of OA are increasing year by year and have become one of the important public health problems facing the world [4]. There is still a lack of targeted OA treatment in part due to a poor understanding of its pathogenesis. Therefore, it is urgent to explore molecular mechanisms underlying OA pathology and define targets for combating this devastating disease.

The risk factors for OA include, but not limited to, aging, joint injury, obesity and heredity [5]. Among them, abnormal mechanical stress is a key risk factor for articular cartilage injury in OA [6–8]. Articular cartilage has the function of bearing and dispersing stress. While normal mechanical loading is known to be important to maintain the structure and the function of articular cartilage, abnormal mechanical stress causes the imbalance of cartilage matrix metabolism and the development of cartilage degeneration, leading to OA injury [9]. As the only cell type in articular cartilage, chondrocytes can convert mechanical stimuli into biochemical signals through mechanotransduction, thus regulating cartilage metabolism [10].

Piezo1 is a large transmembrane protein that is highly conserved among different species. Piezo1 is a key molecule for cells to sense and respond to mechanical stimuli [11–12]. Under stress stimulation, Piezo1 causes Ca²⁺ flow into cells through deformation and then transduces mechanical signals into biochemical and biological signals [13]. Recently, important roles of alterations in Piezo1 expression and activation in bone and cartilage diseases have been implicated by various studies from different groups [14–16]. Abnormal stress activation of Piezo1 leads to decreased chondrocyte activity or death, which is closely related to cartilage damage [17–18]. However, whether or not alterations in Piezo1 expression and activation play a role in OA pathogenesis remains poorly defined.

In this study, we demonstrate that Piezo1 is highly expressed in articular chondrocytes from human OA articular cartilage. Deleting Piezo1 expression in chondrocytes alleviates, while activating Piezo1 aggravates, OA damages in adult mice. We further demonstrate that artemisinin (ART), a potent antimalarial drug, inhibits Piezo1 activation and OA progression in mice.

Materials and Methods

Ethics statement

All experiments involving animals were conducted according to the ethical policies and procedures approved by the Institutional Animal Care and Use Committee (IACUC) of SUSTech (SUSTech-JY202108032). All experiments involving human patients were conducted according to the ethical policies and procedures approved by the Medical Ethical Committee of Linyi People's Hospital (Approval no. YX200278). Informed consent was obtained from each participant.

Human cartilage samples

Human OA cartilage samples were obtained from OA patients underwent total knee replacement surgery in Linyi People's Hospital (56 to 72 years old). We took into account variables, such as the patient's gender, age, obesity, trauma or senility, and whether they had other diseases. Samples from patients with other diseases or significant differences in variables were excluded in this study. The severity of arthritis degeneration was assessed according to the Kellgren-Lawrence grading system [19]. The adjacent healthy cartilage tissues were used as controls. Articular cartilage was decalcified with 15 % EDTA as previously described [5], and paraffin embedded for further Safranin O/Fast Green (SO/FG) and immunofluorescence (IF) staining.

Animals

Piezo 1flox/flox mice were purchased from the Jackson Laboratory (Bar Harbor, ME, USA). Aggrecan^{CreERT2} mice were previously described [5]. Both mice were in stable C57BL/6 background for more than ten generations. To delete Piezo1 in articular chondrocytes, Piezo1^{flox/flox} mice were crossed with Aggrecan^{CreERT2} mice to produce *Piezo1^{flox/flox};Aggrecan^{CreERT2}* mice. 12-week-old *Piezo1^{flox/}* flox: Aggrecan^{CreERT2} mice were divided into two groups, Conditional knockout (cKO) group mice were injected intraperitoneally with tamoxifen (TAM, 1 mg/10 g body weight; Sigma Aldrich) for 5 consecutive days to induce Cre activity, and the other group of mice were injected with the same amount of corn oil as the control group. Mice used in this study were housed under standard conditions in the specific-pathogen-free (SPF) experimental animal center of the Southern University of Science and Technology (SUSTech). To minimize use of mice, only male mice were utilized in experiments in this study. All relevant guidelines for mouse experiments were adhered to in this study.

Dmm-induced OA model in mice

One week after TAM injection, cKO and control mice underwent the destabilization of medial meniscus (DMM) surgery. DMM surgery was performed in the right knees of mice to induce OA lesions according to a protocol previously described [21]. At 8 weeks postoperatively, the mice were euthanized and knee specimens were collected.

Intra-articular administration of Yoda1 in experimental OA

The intra-articular injection of Yoda1 (MCE, HY-18723) or ART (MCE, HY-B0094) was performed as previously described [5]. C57BL/6J mice were given intra-articular injections once a week starting on day 3 post DMM. The mice were euthanized 8 weeks after administration for histological analysis. DMM mice injected with the same amount of solvent were used as control.

Micro-computed tomography

After fixation of the mouse knee joints with 4 % paraformaldehyde, we scanned the specimens using a Skyscan 1276 high-resolution CT scanner (Bruker) with a voltage of 60 kV and 100 μ Amp current, with a resolution of 10 μ M. 3D reconstruction and data analysis were then performed according to our previously established protocol [22].

Animal behavioral tests

The von Frey test was performed as previously described [5]. Briefly, mice were first placed on an elevated mesh platform and acclimated for 15 min in a quiet environment. The hind paw was then dialed from below using calibrated von Frey wire and calculated using an iterative method. Gait analysis was performed to assess pain-related behavior in mice using the Catwalk XT 9.0 system (Noldus Information Technology, Wageningen, the Netherlands). Properly trained mice were individually placed on the glass walkway and allowed to walk back and forth. The footprints were recorded by high-speed cameras located beneath the glass walkway. At 8 weeks under DMM, mice were subjected to gait analysis, and gait parameters, such as stand, swing, footprint area and intensity, were recorded and analyzed [23-24]. The ratio of parameters from right hand to left hand (RH/LH) was calculated for statistical analysis. The animal behavioral tests were performed in a double-blind manner.

Histological analyses

Tissue specimens were fixed in 4 % paraformaldehyde at 4 °C for 24 h, decalcified with 10 % EDTA (pH 7.4) for 2 weeks at 4 °C and paraffin-embedded and 5-µm thick sagittal sections were cut. Hematoxylin-eosin (H/E) and SO/FG staining was performed as previously described [25]. Cartilage degeneration and osteophyte formation were assessed by SO/FG staining using the Osteoarthritis Research Society International (OARSI) scoring system and osteophyte scoring system, respectively. H/E sections were used to assess synovitis through the Krenn's score system. Each section was evaluated in a double-blind manner. For OARSI scoring system [26], score of 0 represents normal cartilage; 0.5 = loss of safranin-O without structural changes; 1 = small fibrillations without loss of cartilage; 2 = vertical clefts and loss of surface lamina; 3 = vertical clefts/erosion to the calcified cartilage lesion extending to < 25 % of the articular surface, 4 = lesion reaches the calcified cartilage for 25-50 % of the articular surface. 5 = lesion reaches the calcified cartilage for 50–75 % of the articular surface, and 6 = lesion reaches the calcified cartilage for > 75 % of the articular surface. For Krenn's synovitis scoring system [27], H/E sections were assessed by scoring the expansion of the synovial lining cell layer, the density of resident cells, and the inflammatory infiltrate, on a scale from 0 to 3 according to severity. The sum of the scores represents the severity of synovitis: 0-1 = no synovitis, 2-4 = low-grade synovitis,

and 5–9 = high-grade synovitis. Osteophyte scores were based on osteophyte size and maturity [28]. Osteophyte size was graded into 4 grades: 0 = none, 1 = slightly increased, 2 = moderately increased, and 3 = significantly increased. Osteophyte maturity was graded into 4 grades: 0 = none, 1 = predominantly cartilage, 2 = mixed cartilage and bone, and 3 = predominantly bone. Each section was evaluated in a double-blind way.

Immunofluorescence and confocal analyses

Specimens were prepared as previously described [29–30]. Sections were antigen-retrieved overnight in sodium citrate buffer, permeabilized with 0.2 % Triton X-100, blocked with 2 % BSA for 1 h, and then incubated with primary antibodies overnight at 4 °C. After washing, sections were incubated with anti-rabbit Alexa Fluor 488 (Invitrogen) or anti-mouse Alexa Fluor 568 (Invitrogen) secondary antibodies (1:400 dilution) for 1 h at room temperature. The fluorescence signal of the region of interest was determined using a confocal microscope (Leica SP8 Confocal Microscopy System). Quantitative analysis of IF staining was performed in a double-blind manner.

Immunohistochemistry

After antigen retrieval, BSA blocking and primary antibody incubation overnight, the tissue sections were incubated with horseradish peroxidase (HRP) coupled with secondary antibody, followed by DAB coloration (Abcam) and hematoxylin restaining. Finally, the images were taken under a microscope. Quantitative analysis was performed in a double-blind manner.

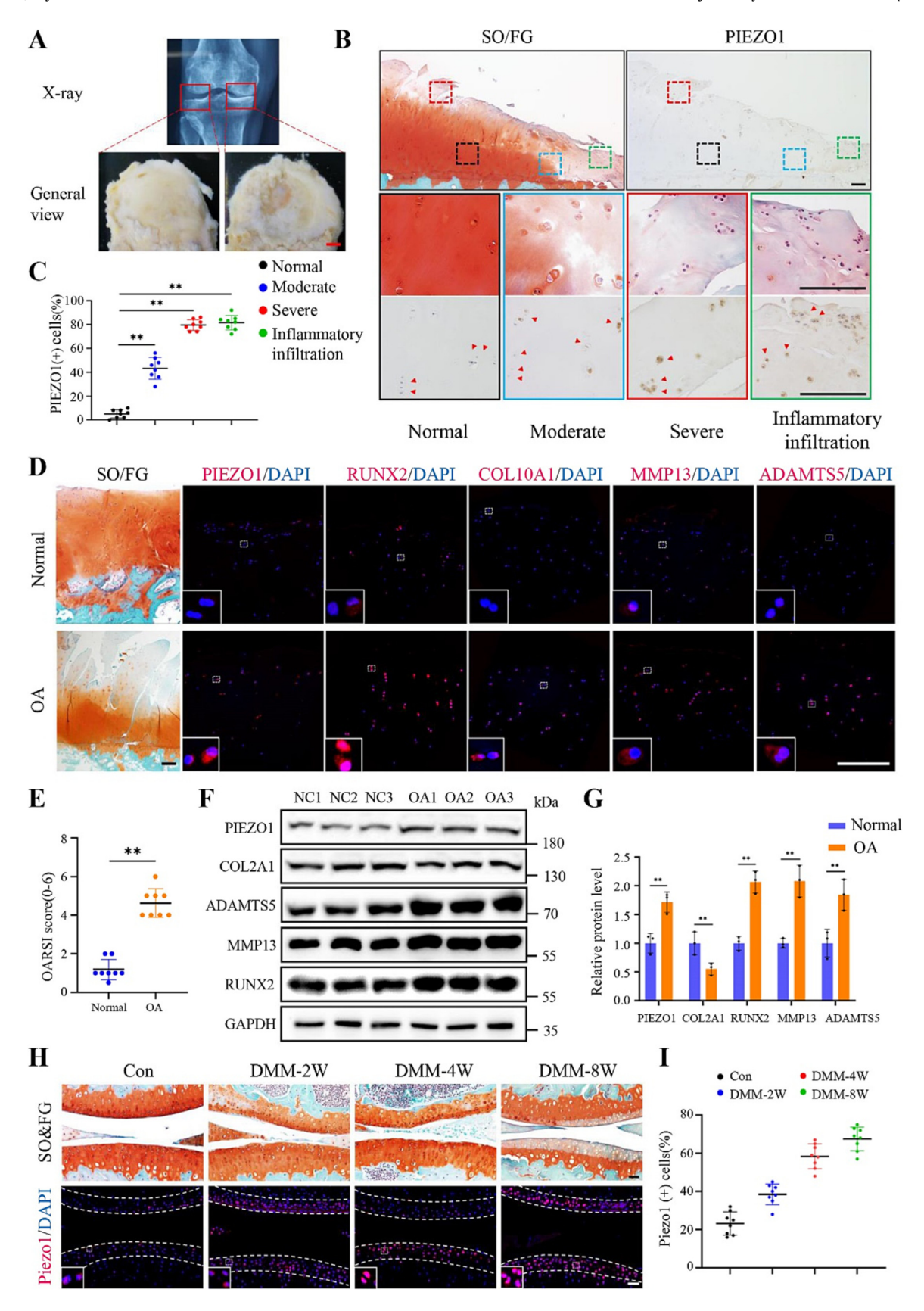
Isolation of human primary articular chondrocytes

Human primary articular chondrocytes (HACs) were isolated from articular cartilage of OA patients underwent total knee replacement. The adjacent healthy cartilage tissues were used as controls. The cartilage tissue samples were rinsed with normal saline during the operation, then placed in PBS containing 1 % penicillin and streptomycin, and moved into a biological safety cabinet for aseptic operation. The articular cartilage was the cut into tiny pieces with scissors, digested with collagenase II for 12 h according to the modified protocol [31], filtered and centrifuged to obtain primary chondrocytes. chondrocytes were cultured in DMEM-F12 medium containing 10 % FBS and 100 IU/ml penicillin/streptomycin in an incubator with 5 % $\rm CO_2$ at 37 °C.

Cell transfection experiments

Small interfering RNA (siRNA) oligonucleotides and untargeted interfering control siRNA for human *PIEZO1* were purchased from GenePharma. OA HACs were seeded in six-well plates at 50 % confluence and transfected with 100 nM siRNA-*PIEZO1* using Lipofectamine™ RNAiMAX (Invitrogen) in Opti MEM (Thermo Fisher Scientific, Inc.), as described in the manufacturer's protocol. 24 h after transfection, the cell culture medium was replaced with fresh DMEM-F12 and cultured for another 48 h. The oligonucleotide sequence of *PIEZO1* siRNA is: For: GGUUCCCACUGCUCUUCAUTT; Rev: AUGAAGAGCAGUGGGAACCTT.

OA HACs were transfected with the indicated pECMV-Piezo1-m-FLAG using Lipofectamine $^{\rm TM}$ 3000 Transfection Reagent (Thermo Fisher Scientific, Inc.) and harvested 48 h after transfection.



Rna-seq analysis

The three biologically independent samples in each group were combined into one, and the total RNA in the samples was extracted with Trizol. The cDNA libraries were constructed using MGIEasy RNA Library Preparation Kit (MGI, CN). After evaluating the quality of the library on Agilent 2100 biological analyzer and transformed by the sequencing platform software to generate the original data. Sequencing data were sequentially filtered by DNBSEQ platform, and reference genes were compared by Bowtie2, then Differentially expressed genes (DEGs) were analyzed using DESeq R package, significantly differential expression was defined as |log2FC| >=1 and false discovery rate (FDR) <=0.01. KEGG enrichment analysis was conducted using cluster Profiler R package.

Western blotting analysis

Western blot analysis was performed as previously described [32]. The cells were lysed with RIPA buffer for 10 min and the protein was extracted. The samples were separated by SDS-PAGE for 90 min and then transferred to PVDF membranes by wet transfer. Each membrane was incubated with primary antibody at 4 °C overnight. After incubation with specific secondary antibodies, proteins were detected with enhanced chemiluminescence kit (ECL kit, Bio-Rad, USA).

Computational protein-ligand docking

The 3D structure of ART was obtained from the PubChem database (https://www.ncbi.nlm.nih.gov/), and the structural energy was minimized in the ChemBioDraw 3D module. The crystal structure of Piezo1 was obtained from the PDB database (https://www.rcsb. org/). AutodockTools was used to process the protein, including hydrogenation, water removal and energy minimization, and other parameters remain at default values. After the grid was defined on the active site of the receptor protein, the docking procedure was performed by AutoDock-Vina to dock the Piezo1 and ART. PyMOL was used to process the results and generate visual graphs.

Calcium imaging

OA HACs were incubated in Fura-2/AM (2 μM, Beyotime Biotechnology) for 30 min and diluted in Ringer's solution (pH = 7.4) containing with 135 mM NaCl, 2 mM CaCl₂, 5.4 mM KCl, 5 mM HEPES and 5.5 mM glucose. Fluorescence of chondrocytes was measured under excitation light of 340 nm and 380 nm (Olympus IX51 with ORCA-R2 digital camera, Hamamatsu Corporation, Japan). The 340/380 nm emission ratio was used to determine the intracellular Ca²⁺ concentration ([Ca²⁺]_i). After the 340/380 nm emission ratio in chondrocytes was stable, Yoda1 was added to activate PIEZO1 to induce intracellular calcium influx, and when the 340/380 nm emission ratio reached a peak, ART (50 μM) was added for intervention, and the 340/380 nm

emission ratio was recorded. The fold change of $[Ca^{2+}]i$ was expressed as the ratio of the 340/380 ratio before and after treatment. Cells with a $[Ca^{2+}]i$ fold change greater than 1.05 were defined as responsive cells.

Statistical analysis

All experiments were performed at least three times. All data were presented as mean \pm standard deviation and analyzed or plotted using GraphPad Prism 8.0. Differences between the two groups were analyzed using Student's t-test. For comparisons between more than two groups, one-way analysis of variance (ANOVA) and Tukey's or Dunnett's multiple comparison test were used. The value of P < 0.05 was considered statistically significant.

Results

Piezo1 expression is upregulated in chondrocytes of human and mouse OA articular cartilage

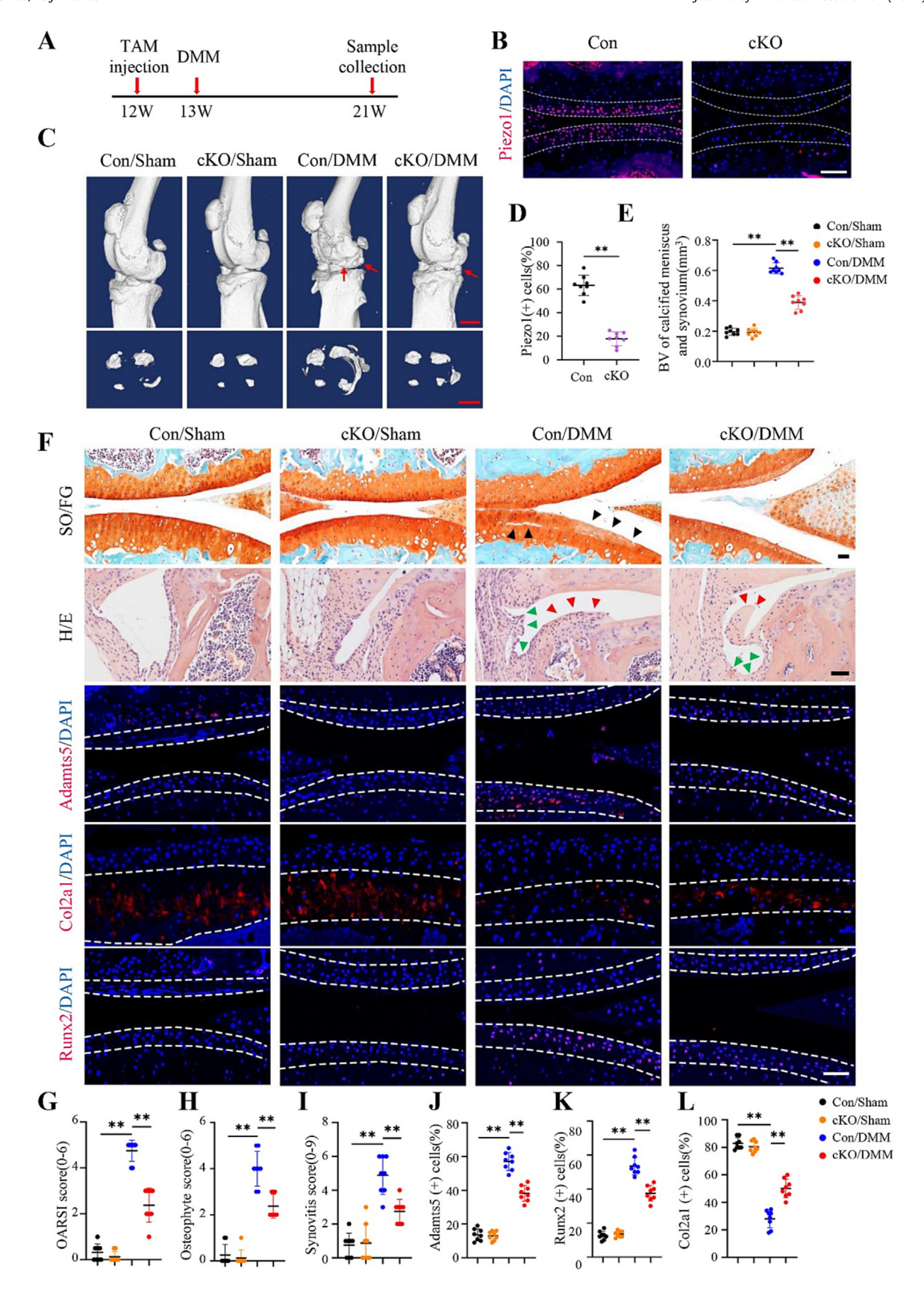
We collected degenerative cartilage tissue samples from 16 knee joints of OA patients undergoing knee replacement (Supplementary Tab. 2). OA cartilage was significantly thinner than healthy cartilage and had reduced proteoglycan (Fig. 1A) and significantly increased OARSI score (Fig. 1E). IHC staining showed that PIEZO1 expression in articular cartilage was significantly increased in the area of cartilage injury and inflammatory infiltration (Fig. 1B, C). Interestingly, in vitro experiments showed that proinflammatory factors, such as IL-1β, IL-6, and LPS, could significantly promote the expression of PIEZO1 in HACs (Supplementary Fig. 2). Further analysis revealed that elevated PIEZO1 level in cartilage of OA patients was consistent with the expression levels of OA-related proteins, such as RUNX2, COL10A1, ADAMTS5 and MMP13, which was further confirmed by western blotting analysis of HACs in vitro (Fig. 1D, F-G). The percentages of Piezo1-positive articular chondrocytes were significantly increased in a timedependent manner after DMM surgery (Fig. 1H, I).

Piezo1 deletion in articular chondrocyte attenuates DMM-induced OA lesions in mice

We next determined the effects of Piezo1 deletion in articular chondrocytes on DMM-induced OA lesions in adult mice. We crossed the *Piezo1*^{foxl/flox} mice with the *Aggrecan*^{CreERT2} mice to obtain *Piezo1*^{floxl/flox}; *Aggrecan*^{CreERT2} mice and the genotypes were verified by PCR analysis using tail DNA (Supplementary Fig. 3A, B). At 12 weeks of age, TAM was injected into the *Piezo1*^{flox/flox}; *Aggrecan*^{CreERT2} mice to induce Cre expression and deletion of Piezo1(Fig. 2A). The results showed that the expression of Piezo1 protein was dramatically reduced in chondrocytes of the knee joint articular cartilage in cKO mice, as revealed by IF staining (Fig. 2B, D). At 8 weeks under DMM surgery, μCT analysis was performed in the knee joints of mice and revealed that the degrees of menis-



Fig. 1. Piezo1 expression is upregulated in chondrocytes of human and mouse OA articular cartilage. (A) Representative X-ray and general views of knee joints of OA patients with total knee arthroplasty, with red boxes indicating respective healthy and OA areas. Scale bar: 1 cm. (B) Representative immunohistochemical images of safranin O/fast green (SO/FG) and PIEZO1 in OA cartilage with different degrees of injury. The images with higher magnification in different colors at the bottom are the corresponding areas in the dashed boxes of the upper images. Scale bar: 200 μ m. (C) Quantitative analysis PIEZO1-positive chondrocytes as a proportion of the total chondrocytes in cartilage with different degrees of injury. N = 8 per group. (D) Representative images of SO/FG staining and immunofluorescence (IF) of PIEZO1, RUNX2, COL10A1, MMP13 and ADAMTS5 in normal and OA cartilages. Scale bar: 200 μ m. (E) OARSI score of normal and OA cartilages. (F, G) Western blotting and Quantification of PIEZO1, COL2A1, ADAMTS5, MMP13 and RUNX2 in normal and OA primary articular chondrocytes. N = 3 biologically independent replicates per group. (H) Representative images of SO/FG staining and IF of Piezo1 in chondrocytes of controls and mice at 2, 4 and 8 weeks after DMM surgery, white dashed lines indicate the cartilage surfaces. Scale bar: 50 μ m. (I) Quantification of PIEZO1-positive chondrocytes based on staining results in (H). N = 8 biologically independent replicates per group. Results were expressed as mean \pm standard deviation (s.d.). **P < 0.01. (For interpretation of the references to colour in this figure legend, the reader is referred to the web version of this article.)



cus ossification and osteophyte formation of the knee joints were significantly lower in DMM cKO mice than those in DMM control mice (Fig. 2C, E). There was no significant difference between control and cKO mice with sham surgeries (Fig. 2C, E). Histological analyses revealed that DMM cKO mice exhibited significant reductions in cartilage erosion, proteoglycan loss, osteophyte and synovial formation and an increase in OARSI score in articular cartilage compared with those in DMM control mice (Fig. 2F-I). Again, no marked differences were observed in these parameters between control and cKO mice with sham surgeries (Fig. 2F-I). IF staining showed that the numbers of Runx2- and Adamts5positive cells were significantly decreased in the articular cartilage of cKO mice relative to those in control mice, while the expression level of Col2a1 was higher in cKO mice than that of the control mice. Note: there were no significant differences between control and cKO mice with sham surgeries (Fig. 2F. I-L).

Activation of Piezo1 induces metabolic disorder of chondrocytes and exacerbates OA development in mice

We further investigated the effects of Piezo1 activation on DMM-induced OA damages in mice. To this end, DMM mice were given intra-articular injection of Yoda1, a selective activator of Piezo1. The results showed that Yoda1 treatment markedly exacerbated the OA lesions in the knee joints in DMM mice (Fig. 3). While Yoda1 treatment did not cause marked OA lesions in sham mice, it significantly aggravated the meniscal ossification, osteophyte formation, cartilage erosion, loss of proteoglycans and expression of OA-related genes, such as Runx2 and Adamts5, in DMM mice (Fig. 3B-K).

PIEZO1 activation promotes catabolism but inhibits anabolism in articular chondrocytes in a PI3K-AKT-dependent manner

We next determined the direct effects of modulation of PIEZO1 expression and activation in primary human articular chondrocytes (HACs) (Supplementary Tab. 3). Results from RNAseq analyses showed that PI3K/AKT or MAPK signaling pathways were largely modulated by siRNA knockdown (Fig. 4A), activation (Fig. 4B) or overexpression of Piezo1 (Fig. 4C) in OA HACs. Furthermore, siRNA knockdown of PIEZO1 expression significantly decreased the protein levels of RUNX2 and catabolic enzyme MMP13 and increased that of anabolic COL2A1 in OA HACs (Fig. 4D, E). In contrast, the PIEZO1 activator Yoda1 exerted opposite effects in OA HACs, which were reversed by inhibition of PI3K-AKT but not p38 MAPK (Fig. 4F, G). Yoda1 increased the protein levels of p-PI3K and p-AKT without markedly affecting their total protein levels, while si-PIEZO1 exerted opposite effects on both pathways in OA HACs (Fig. 4H-K). Interestingly, we found that Yoda1 treatment did not increase expression of RUNX2 and MMP13 and decreased that of COL2A1 in healthy HACs (Supplementary Fig. 4). Similarly, Piezo1 deletion reduced, while Yoda1

increased, the level of p-AKT protein in articular cartilage of mice (Fig. 4L).

Artemisinin suppresses the PIEZO1-mediated calcium flux and reverses OA-related gene expression induced by PIEZO1 activation

In an effort to define PIEZO1-targeting drugs for potential OA treatment, via literature research and virtual docking technology, we found that artemisinin (ART), a potent antimalarial drug, may be a PIEZO1-targeting drug. Computer protein-ligand docking simulation revealed several amino acid residues near the ion channel pore of Piezo1 molecule with strong binding ability to ART (Supplementary Fig. 5 A,B) [31]. Results from in vitro studies showed that ART preincubation essentially abolished the increases in calcium influx induced by Yoda1 in primary chondrocytes isolated from the knee joint articular cartilage of OA patients (OA HACs) (Fig. 5B) and in cell lines, including the human umbilical vein endothelial cells (HUVECs) (Fig. 5C), mouse chondrocyte-like ATDC5 cells (Fig. 5D) and murine MLO-Y4 osteocyte-like cells (Fig. 5E). Yoda1 greatly increased the calcium influx in OA HACs, which was dramatically reduced by addition of ART (Fig. 5F). Note: ART at the experimental concentration (50 μ M) did not impact the cell viability (Fig. 5G). Results from RNAseq analysis indicated that ART reversed the effect of Yoda1 by interfering with the PI3K/AKT pathway (Fig. 5H). Yoda1-induced upregulation of RUNX2 and MMP13 and downregulation of COL2A1 in OA HACs were significantly reduced by ART treatment (Fig. 5I, K-N). Results from in vitro experiments confirmed that ART decreased the Yoda1induced increases in the levels of p-PI3K and p-AKT proteins in OA HACs (Fig. 5J, O-P).

ART ameliorates OA lesions caused by Piezo1 activation in mice

Finally, we determined the effects of ART on the OA damages induced by Piezo1 activation in DMM mice. In these experiments, C57BL/6J mice were randomly divided into four groups as indicated. At two months after DMM operation, the DMSO group showed obvious pain-related gait abnormalities and OA pathological features, such as cartilage degeneration, osteophyte formation and synovial infiltration (Fig. 6B-D, Supplementary Fig. 6). When compared with control mice, the ART-treated mice displayed marked ameliorations in articular cartilage erosion, proteoglycan loss, synovial and osteophyte hyperplasia, pain, and expression of OA-related genes (Fig. 6B-L, Supplementary Fig. 6). As expected, Yoad1 treatment increased the values of all above OA-related parameters (Fig. 6B-L). Importantly, Yoda1-induced increases in the OA-related pain, cartilage loss, osteophyte formation and synovitis were dramatically reduced or completely abolished by ART treatment (Fig. 6B-I. Supplementary Fig. 6). At the molecular level. Yoda1-induced decrease in expression of Col2a1 and increases in expression of Runx2 and Adamts5 were largely reversed by ART treatment (Fig. 6E, K-L).



Fig. 2. Piezo1 deletion in articular chondrocyte attenuates DMM-induced OA lesions in mice. (**A**) Schematic diagram illustrating the experimental design. (**B,D**) Representative images of IF staining of Piezo1 in articular cartilage of cKO and Control mice at 2 months after TAM induction. N = 8 biologically independent replicates per group. Scale bar: 100 μm. Quantitative data are shown in D. (**C**) Three-dimensional reconstruction from μCT scans of knee joints from control and cKO mice at 8 weeks after sham or DMM surgery. Scale bar, 1.0 mm. (**E**) The bone volume (BV) of calcified meniscus and synovial tissue was analyzed by μCT. N = 8 biologically independent replicates per group. (**F**) Representative images of SO/FG staining (first row) and hematoxylin-eosin(H/E) staining (second row) of knee joints, and IF staining of Adamts5, Col2a1 and Runx2 (rest rows) in chondrocytes of cKO and Controls at 8 weeks after DMM surgery. Black arrowheads show cartilage damage, green arrowheads show marked synovial hyperplasia, red arrowheads show marked hyperplastic osteophyte, white dashed lines indicate the cartilage surfaces. Scale bar: 50 μm. (**G-L**) OARSI score(G), osteophyte score (H), synovitis score (I) and quantification of Adamts5(J), Runx2(K) and Col2a1(L) positive chondrocytes based on staining results in (F). N = 8 biologically independent replicates per group. Results were expressed as mean ± standard deviation (s.d.). **P < 0.01. (For interpretation of the references to colour in this figure legend, the reader is referred to the web version of this article.)

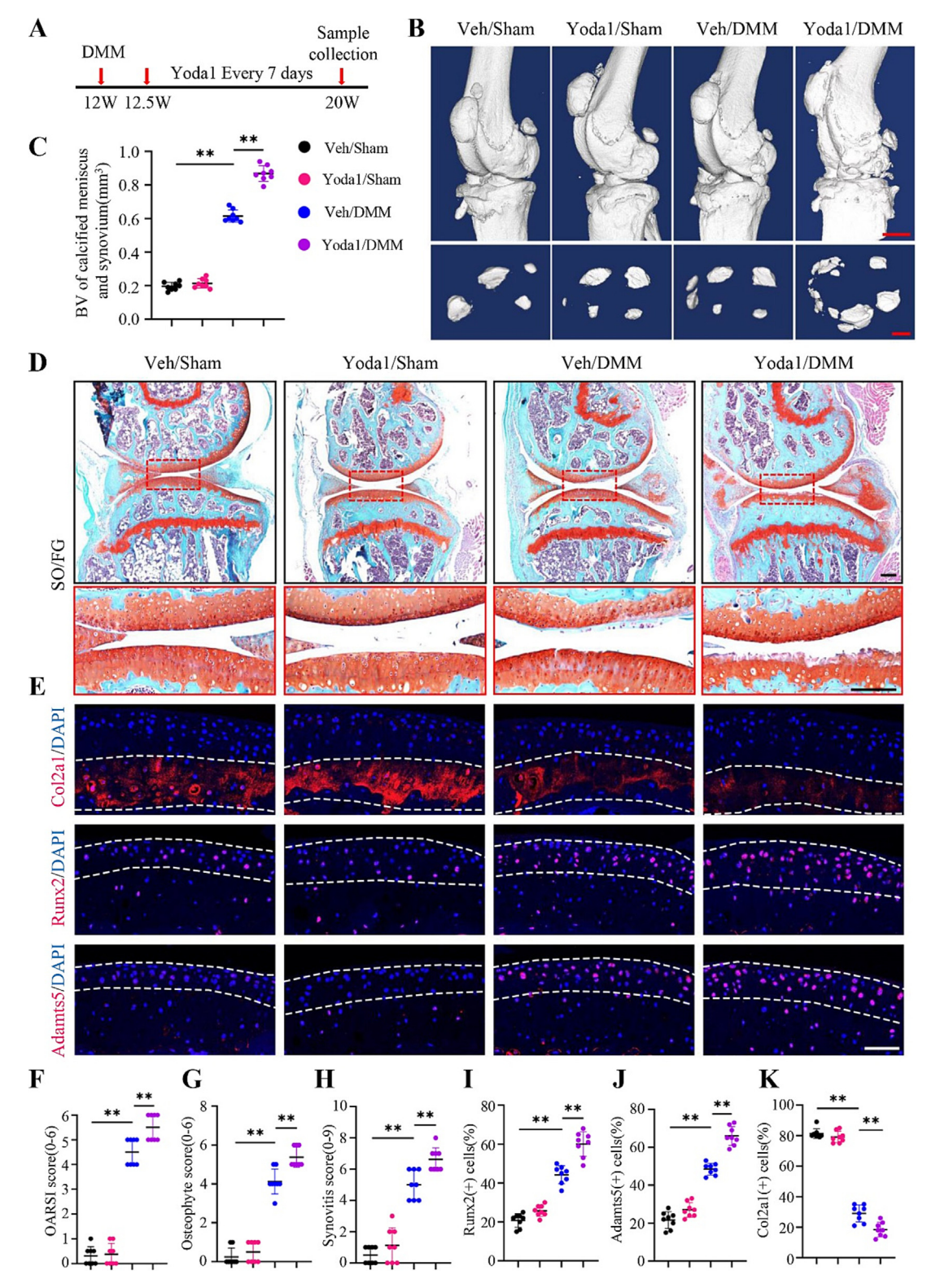


Fig. 3. Activation of Piezo1 induces metabolic disorder of chondrocytes and exacerbates OA development in mice. (A) Schematic diagram illustrating the experimental design. On the 3rd day after DMM, mice in the Yoda1 group were injected with Yoda1 dissolved in DMSO (150 μ g/ml, 2 μ l/time, once a week) into the knee joint cavity. Mice in the control group were injected with DMSO at the same time point in the knee joint cavity, and the samples were collected 8 weeks after DMM operation. (B) Three-dimensional reconstruction from μ CT scans of knee joints from Veh and Yoda1 group mice at 8 weeks after sham or DMM surgery. Scale bar, 1.0 mm. (C) The BV of calcified meniscus and synovial tissue was analyzed by μ CT. N = 8 biologically independent replicates per group. (D) Representative SO/FG staining images in articular cartilage of cKO and Control mice at 8 weeks after sham or DMM surgery. The images with higher magnification at the bottom are the corresponding areas in the dashed boxes of the upper images. Scale bar, 200 μ m. (E) Representative images of IF staining of Col2a1, Runx2 and Adamts5 in chondrocytes of Yoda1 and Controls at 8 weeks after DMM surgery, white dashed lines indicate the cartilage surfaces. Scale bar, 50 μ m. (F-K) OARSI score (F), osteophyte score (G), synovitis score (H) and quantitative data of expression of Runx2(I), Adamts5(J) and Col2a1(K) based on staining results in (D, E). N = 8 biologically independent replicates per group. Results were expressed as mean \pm standard deviation (s.d.).

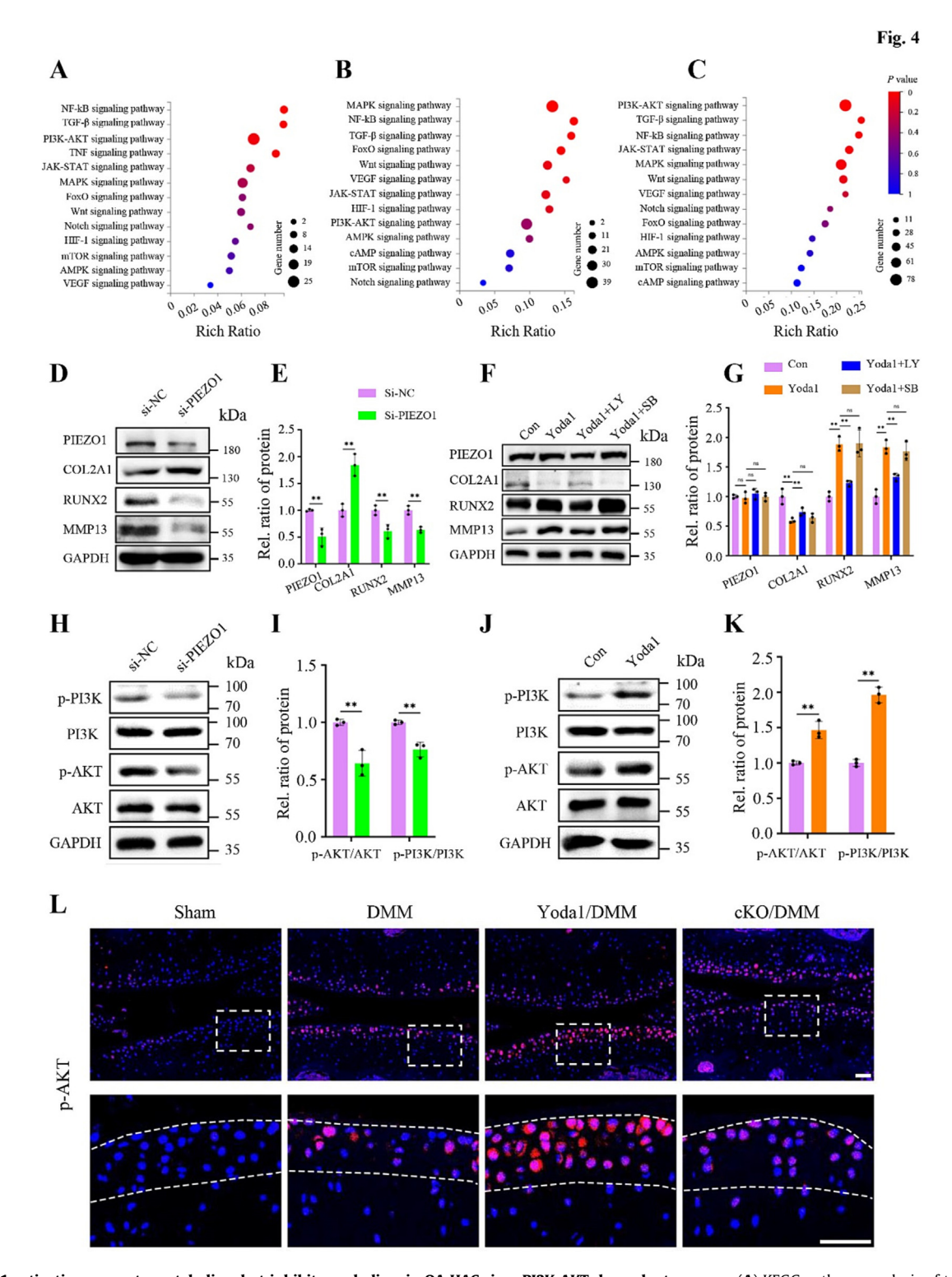


Fig. 4. PIEZO1 activation promotes catabolism but inhibits anabolism in OA HACs in a PI3K-AKT-dependent manner. (A) KEGG pathway analysis of transcripts from experiments of si-NC- and si-PIEZO1-treated OA HACs. (B) KEGG pathway analysis of transcripts from experiments of control and Yoda1 (1 μM) treatment. (C) KEGG pathway analysis of transcripts from experiments of control and overexpression-PIEZO1 in OA HACs. (D) Western blot of PIEZO1, COL2A1, RUNX2 and MMP13 in OA HACs transfected with si-NC and si-PIEZO1 for 48 h. (E) Quantification of (D). (F) Western blot of PIEZO1, COL2A1, RUNX2 and MMP13 in OA HACs treated with Yoda1 with and without LY294002(PI3K inhibitor), SB239063(p38 MAPK inhibitor) for 24 h. (G) Quantification of (F). (H) Western blot of p-PI3K, PI3K, p-AKT and AKT in OA HACs treated with Yoda1 for 30 min. (K) Quantification of (J). All experiments were repeated at least three times independently with similar results. (L) Representative images of IF staining of p-AKT in chondrocytes of cKO, Yoda1 and Controls mice at 8 weeks after DMM surgery, white dashed lines indicate the cartilage surfaces. Scale bar, 50 μm. Results were expressed as mean ± standard deviation (s.d.). **P < 0.01.



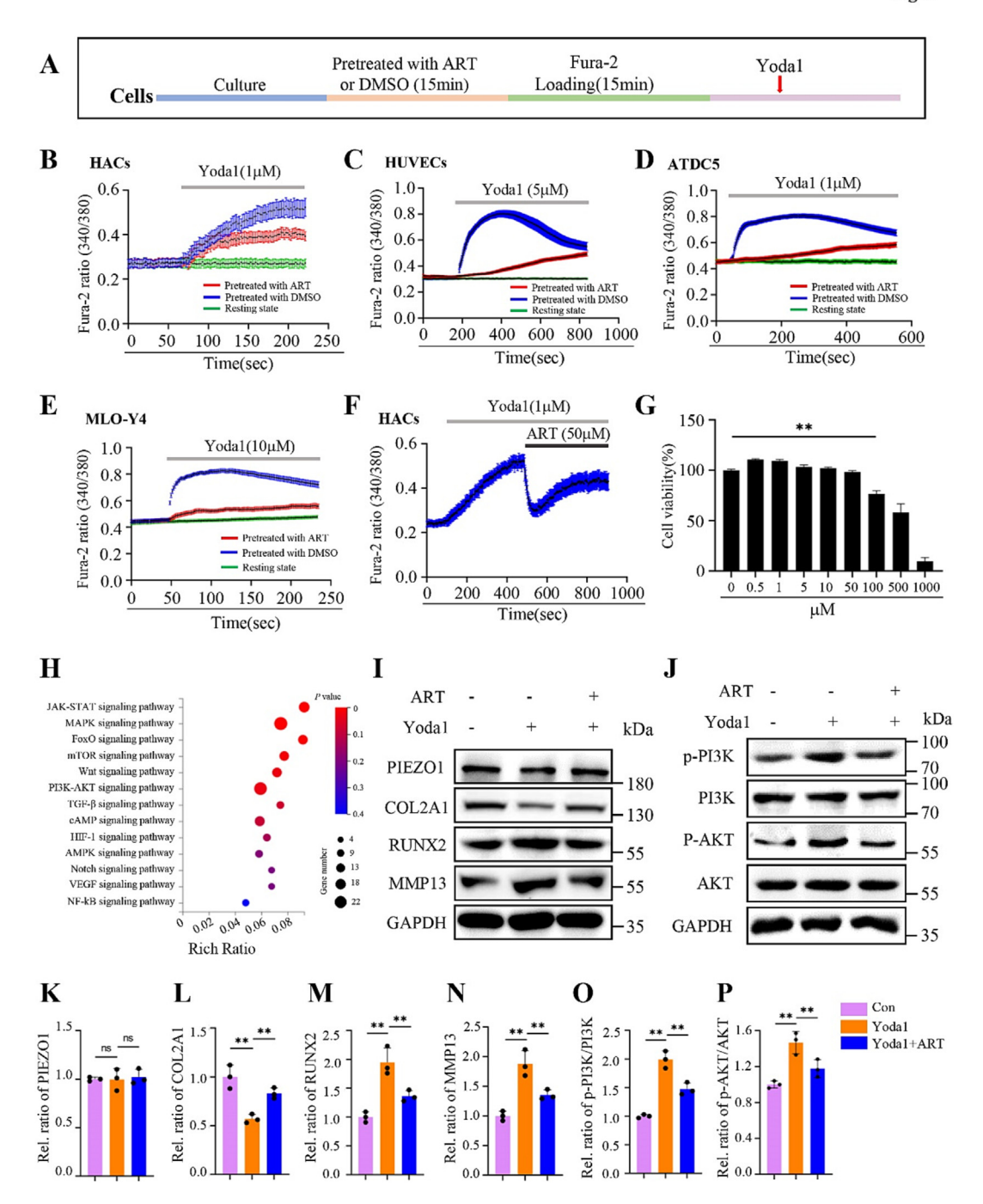
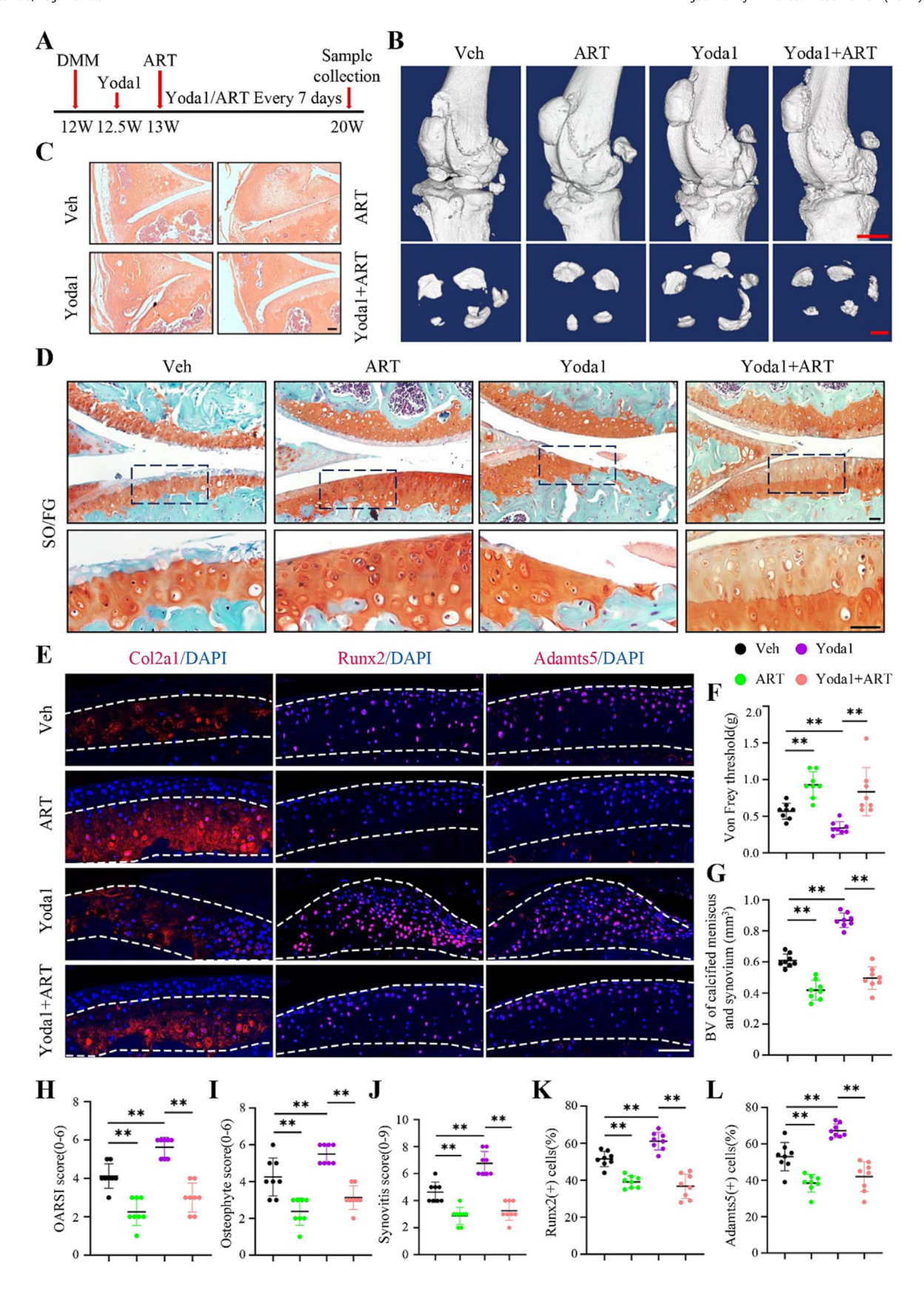


Fig. 5. ART suppresses the PIEZO1-mediated calcium influx and reverses OA-related gene expression induced by PIEZO1 activation. (A) Schematic diagram of experimental design. (B) Representative Fura-2 ratio (340/380) traces obtained from single-cell Ca²⁺ imaging of OA HACs in response to the indicated conditions as shown in (A) (N = 82 cells). (C) Representative Fura-2 ratio (340/380) traces obtained from single-cell Ca²⁺ imaging of HUVECs in response to the indicated conditions as shown in (A) (N = 30 cells). (D) Representative Fura-2 ratio (340/380) traces obtained from single-cell Ca²⁺ imaging of ATDC5 cells in response to the indicated conditions as shown in (A) (N = 52 cells). (E) Representative Fura-2 ratio (340/380) traces obtained from single-cell Ca²⁺ imaging of MLO-Y4 cells in response to the indicated conditions as shown in (A) (N = 40 cells). (F) Single-cell Fura-2 Ca²⁺ imaging experiments showing the average response of OA HACs treated with Yoda1 and ART in turn. (N = 82 cells). The black trace represents the average response of 3-dish repeats. Error bars are shown in colors. Note: ART at the experimental concentration did not impact the cell viability. (G) CCK8 assay was used to detect the effects of different concentrations of ART on OA HACs proliferation. The black trace represents the average response of 3-dish repeats. Error bars are shown in colors. (H) KEGG pathway analysis of transcripts from experiments of Yoda1 and Yoda1 + ART. The three biologically independent samples in each group were combined into one. (I) Western blot of PIEZO1, COL2A1, RUNX2 and MMP13 in OA HACs treated with Yoda1 with and without ART for 20 min. (K-N) Quantification of (J). (O, P) Quantification of (J). All experiments were repeated at least three times independently with similar results. Results were expressed as mean ± standard deviation (s.d.). **P < 0.01.



Discussion

In this study, we demonstrate a critical role of the mechanosensitive channel Piezo1 in promoting OA development and progression. We provide strong evidence from genetic mouse models showing that loss of Piezo1 expression in articular chondrocytes significantly protects against the DMM-induced OA lesions. The loss of Piezo1 ameliorates the articular cartilage damage, meniscus ossification, osteophyte formation, synovitis and OA pain in DMMtreated mice. At the molecular level, Piezo1 loss largely reduces the expression levels of Runx2 and its downstream Adamts5, both well-known factors in OA pathogenesis, in articular chondrocytes [33]. This contributes to the ameliorating effects of Piezo1 loss on the OA lesions. In contrast, the knee joint local activation of Piezo1 via intra-articular injection of Yoda1 exacerbates OA lesions induced by DMM in adult mice. At the molecular level, PIEZO1 regulates expression of RUNX2 and catabolic enzymes in primary OA HACs in a PI3K-AKT dependent manner. Collectively, these results together with our finding that expression of PIEZO1 protein is largely up-regulated in human OA chondrocytes support the notions that PIEZO1 plays an important role in OA pathogenesis and that modulating PIEZO1 expression and activation may be a novel strategy to treat OA.

It is widely believed that DMM induces OA lesions by creating instability of the knee joint and thereby producing imbalanced and abnormal mechanical stress to the joint. Thus, our results suggest that Piezo1 mediates the pathogenesis of mechanical loading-induced OA. Consistently, compressive stress induces Piezo1 expression in articular chondrocytes [18]. In addition, the inflammatory factor IL-1 α also promotes Piezo1 expression through the p38 pathway in chondrocytes [34]. Our in vitro studies show that IL-1 β , IL-6, and LPS elevate the level of Piezo1 protein in primary HACs. Thus, it is interesting to investigate whether Piezo1 is also involved in pathogenesis of other OAs, such as the aging-related OA.

While previous studies have shown that ART can protect the function of chondrocytes under inflammatory stimulation and inhibit the progression of OA [35–36], underlying mechanisms are poorly understood. In this study, we find that ART can effectively inhibit the calcium flux, p-PI3K and p-AKT levels, and expression of catabolism-related protein markers in chondrocytes caused probably by activation of Piezo1. ART not only protects against DMM-induced OA injury in mice, but also improves the pathological changes of OA induced by Yoda1, indicating that ART exerts its anti-OA function at least partially by targeting Piezo1.

In their manuscript, Young, C. et al. reported a limited role of Piezo1/2 proteins in articular cartilage development and OA progression. In their study, the authors deleted expression of both Peizo1 and Piezo2 using the *Gdf5-Cre* transgenic mice and did not observe any marked differences in the severity of OA lesions induced by DMM between control and KO mice [37]. The discrep-

ancy between results of our and their studies could be due to different Cre transgenic mice used to delete Piezo expression (i.e., Aggrecan-CreERT2 in our study vs. Gdf5-Cre in their study). The chondrocytes targeted by Aggrecan-CreERT2 and Gdf5-Cre are not identical in terms of their developmental and differentiation stages and other properties. In addition, the additional deletion of Piezo2 in their mice could also explore the difference. Lee et al. showed that down-regulation of Piezo1 and Piezo2 expression can inhibit chondrocyte death induced by mechanical stress [18]. In this study, we clearly show that Piezo1 loss in Aggrecan-expressing chondrocytes protects against the DMM-induced OA lesions in adult mice.

While ART is a potent antimalarial drug, its mechanism remains poorly understood. Previous studies have shown that ART can be activated by heme and bivalent iron ions, which causes production of free radicals, resulting in damage of malaria parasites [38]. ART was reported to treat malaria by targeting specific proteins, such as PI3K and PfATP6 [39]. In our in vivo and in vitro experiments, we found that ART affected the phosphorylation of PI3K/AKT by suppressing the calcium influx caused by the activation of Piezo1. It would be interesting to investigate whether the antimalarial effect of ART is in part through Piezo1 inhibition. If this is the case, the knowledge from this study will provide new molecular insight for developing new antimalarial drugs.

Our results showed that conditional deletion of Piezo1 or Piezo1 activation via Yoda1 without destabilization (DMM) did not cause OA-like lesions in mice. This may suggest that Piezo1 activation may just be an aggravating factor in OA development. In the future, it will be interesting to determine that Piezo1 activation can impact OA lesions in other OA models without DMM, including the aging-related OA model.

Data sharing statement

All data generated for this study are available from the corresponding authors upon reasonable request.

Compliance with Ethics Requirements

All animal experiments in this study were performed in accordance with institutional guidelines and approved by the Laboratory Animal Centre of Southern University of Science and Technology (SUSTech-JY202108032). Patients involved in the study provided consent, and the study was approved by medical ethics regulations of the Medical Ethical Committee of Linyi People's Hospital (No. YX200278).

Declaration of Competing Interest

The authors declare that they have no known competing financial interests or personal relationships that could have appeared to influence the work reported in this paper.

4

Fig. 6. ART ameliorates OA lesions caused by Piezo1 activation in mice. (**A**) Schematic diagram illustrating the experimental design. On the 3rd day after DMM, mice in the Yoda1 group were injected with Yoda1 dissolved in DMSO (150 μg/ml, 2 μl/time, once a week) into the knee joint cavity, and the mice in the ART group were injected into the joint cavity with ART dissolved in DMSO (1 mM, 2 μl/time, once a week) 7 days after DMM operation. The control group mice were injected with DMSO at the same time point in the knee joint cavity, and the samples were collected 8 weeks after DMM operation. (**B**) Representative 3D reconstruction derived from μCT scans of knee joints from Yoda1-treated mice and controls with or without ART treatment at 8 weeks after DMM surgery. Scale bar, 1.0 mm. (**C**) Representative H/E staining images in articular cartilage of four group mice at 8 weeks after DMM surgery. Scale bar, 50 μm. (**D**) Representative SO/FG staining images in articular cartilage of four group mice at 8 weeks after DMM surgery. The enlarged images at the bottom are the corresponding areas in the dashed boxes of the upper images. Scale bar, 50 μm. (**E**) Representative IF staining images of Col2a1, Runx2, Adamts5 in chondrocytes of DMM joint sections, white dashed lines indicate the cartilage surfaces. Scale bar, 50 μm. (**F**) Results of Von Frey test. (**G**) The BV of calcified meniscus and synovial tissue was analyzed by μCT. N = 8 biologically independent replicates per group. (**H-L**) OARSI score(H), osteophyte score (I), synovitis score (J) and quantification of Runx2 (K) and Adamts5 (L) positive chondrocytes based on SO/FG and IF staining results in (D, E). N = 8 biologically independent replicates per group. Results were expressed as mean ± standard deviation (s.d.). ***P < 0.01.

Acknowledgments

The authors acknowledge the assistance of Core Research Facilities of Southern University of Science and Technology. This work was supported, in part, by the Shenzhen Fundamental Research Program (JCYJ20220818100617036), the National Key Research and Development Program of China Grants (2019YFA0906004), the National Natural Science Foundation of China Grants (82261160395, 82230081, 82250710175, 81991513, 81870532), the Guangdong Provincial Science and Technology Innovation Council Grant (2017B030301018), the Shenzhen Key Microenvironment Laboratory of Cell (ZDSYS20140509142721429), the Shenzhen Stable Support Plan Program for Higher Education Institutions (20200925150409001), the China Postdoctoral Science Foundation (2022M711499), the Youth Project of Natural Science Foundation of Shandong Province (ZR2021QH230) and the Joint Foundation Project of Natural Science Foundation of Shandong Province (ZR2022LZY002).

Appendix A. Supplementary material

Supplementary data to this article can be found online at https://doi.org/10.1016/j.jare.2023.09.040.

References

- [1] Sharma L. Osteoarthritis of the Knee. N Engl J Med. 2021;384(1):51-59.
- [2] Long H, Liu Q, Yin H, et al. Prevalence Trends of Site-Specific Osteoarthritis From 1990 to 2019: Findings From the Global Burden of Disease Study 2019. Arthritis Rheumatol 2022;74(7):1172–83.
- [3] Abramoff B, Caldera FE. Osteoarthritis: Pathology, Diagnosis, and Treatment Options. *Med Clin North Am.* 2020;104(2):293-311.
- [4] Hunter DJ, Bierma-Zeinstra S Osteoarthritis. Lancet 2019;393 (10182):1745-59.
- [5] Wu X, Lai Y, Chen S, et al. Kindlin-2 preserves integrity of the articular cartilage to protect against osteoarthritis. Nat Aging 2022;2(4):332–47.
- [6] Bannuru RR, Osani MC, Vaysbrot EE, et al. OARSI guidelines for the non-surgical management of knee, hip, and polyarticular osteoarthritis. Osteoarthritis Cartilage 2019;27(11):1578–89.
- [7] Zeng CY, Zhang ZR, Tang ZM, Hua FZ. Benefits and Mechanisms of Exercise Training for Knee Osteoarthritis. Front Physiol 2021;12:794062.
- [8] Chen S, He T, Zhong Y, et al. Roles of focal adhesion proteins in skeleton and diseases. Acta Pharm Sin B 2023;13(3):998–1013.
- [9] Heijink A, Vanhees M, van den Ende K, et al. Biomechanical considerations in the pathogenesis of osteoarthritis of the elbow. Knee Surg Sports Traumatol Arthrosc 2016;24(7):2313–8.
- [10] Zhao Z, Li Y, Wang M, Zhao S, et al. Mechanotransduction pathways in the regulation of cartilage chondrocyte homoeostasis. J Cell Mol Med 2020;24:5408–19.
- [11] Coste B, Mathur J, Schmidt M, et al. Piezo1 and Piezo2 are essential components of distinct mechanically activated cation channels. Science 2010;330(6000):55–60.
- [12] Qin L, He T, Chen S, et al. Roles of mechanosensitive channel Piezo1/2 proteins in skeleton and other tissues. Bone Res 2021;9(1):44.
- [13] Qin L, Liu W, Cao H, et al. Molecular mechanosensors in osteocytes. Bone Res 2020;8:23.
- [14] Wang L, You X. Lotinun S, at al. Mechanical sensing protein PIEZO1 regulates bone homeostasis via osteoblast-osteoclast crosstalk. Nat Commun 2020;11 (1):282.

- [15] Wu J, Chen Y, Liao Z, et al. Self-amplifying loop of NF-κB and periostin initiated by PIEZO1 accelerates mechano-induced senescence of nucleus pulposus cells and intervertebral disc degeneration. Mol Ther 2022;30(10):3241–56.
- [16] Jones RC, Lawrence KM, Higgins SM, et al. Urocortin-1 Is Chondroprotective in Response to Acute Cartilage Injury via Modulation of Piezo1. Int J Mol Sci 2022;23(9):5119.
- [17] Ren X, Li B, Xu C, et al. High expression of Piezo1 induces senescence in chondrocytes through calcium ions accumulation. Biochem Biophys Res Commun 2022;607:138–45.
- [18] Lee W, Leddy HA, Chen Y, et al. Synergy between Piezo1 and Piezo2 channels confers high-strain mechanosensitivity to articular cartilage. Proc Natl Acad Sci U S A 2014;111(47):E5114–22.
- [19] Kohn MD, Sassoon AA, Fernando ND. Classifications in Brief: Kellgren-Lawrence Classification of Osteoarthritis. Clin Orthop Relat Res 2016;474 (8):1886–93.
- [21] Li J, Zhang B, Liu WX, et al. Metformin limits osteoarthritis development and progression through activation of AMPK signalling. Ann Rheum Dis 2020;79 (5):635–45.
- [22] Huang J, Zhao L, Fan Y, et al. The microRNAs miR-204 and miR-211 maintain joint homeostasis and protect against osteoarthritis progression. Nat Commun 2019;10(1):2876.
- [23] Timotius IK, Moceri S, Plank AC, et al. Silhouette-Length-Scaled Gait Parameters for Motor Functional Analysis in Mice and Rats. eNeuro 2019;6 (6). ENEURO.0100-19.2019.
- [24] Lakes EH, Allen KD. Gait analysis methods for rodent models of arthritic disorders: reviews and recommendations. Osteoarthritis Cartilage 2016;24 (11):1837–49.
- [25] Chen S, Wu X, Lai Y, et al. Kindlin-2 inhibits Nlrp3 inflammasome activation in nucleus pulposus to maintain homeostasis of the intervertebral disc. Bone Res 2022;10(1):5.
- [26] Glasson SS, Chambers MG, Van Den Berg WB, Little CB. The OARSI histopathology initiative - recommendations for histological assessments of osteoarthritis in the mouse. Osteoarthritis Cartilage 2010;18(Suppl 3):S17–23.
- [27] Krenn V, Morawietz L, Burmester GR, et al. Synovitis score: discrimination between chronic low-grade and high-grade synovitis. Histopathology 2006;49 (4):358–64.
- [28] Zhang H, Shao Y, Yao Z, et al. Mechanical overloading promotes chondrocyte senescence and osteoarthritis development through downregulating FBXW7. Ann Rheum Dis 2022;81(5):676–86.
- [29] Cao H, Yan Q, Wang D, et al. Focal adhesion protein Kindlin-2 regulates bone homeostasis in mice. Bone Res 2020;8:2.
- [30] Lai Y, Zheng W, Qu M, et al. Kindlin-2 loss in condylar chondrocytes causes spontaneous osteoarthritic lesions in the temporomandibular joint in mice. Int | Oral Sci 2022;14(1):33.
- [31] Wang, Y., et al. A lever-like transduction pathway for long-distance chemicaland mechano-gating of the mechanosensitive Piezo1 channel. Nat Commun 9, 1300 (2018).
- [32] Fu X, Zhou B, Yan Q, et al. Kindlin-2 regulates skeletal homeostasis by modulating PTH1R in mice. Signal Transduct Target Ther 2020;5(1):297.
- [33] Chen D, Kim DJ, Shen J, et al. Runx2 plays a central role in Osteoarthritis development. J Orthop Translat 2019;23:132–9.
- [34] Lee W, Nims RJ, Savadipour A, et al. Inflammatory signaling sensitizes Piezo1 mechanotransduction in articular chondrocytes as a pathogenic feed-forward mechanism in osteoarthritis. Proc Natl Acad Sci U S A 2021;118(13): e2001611118.
- [35] Zhong G, Liang R, Yao J, et al. Artemisinin Ameliorates Osteoarthritis by Inhibiting the Wnt/β-Catenin Signaling Pathway. Cell Physiol Biochem 2018;51(6):2575–90.
- [36] Li J, Jiang M, Yu Z, et al. Artemisinin relieves osteoarthritis by activating mitochondrial autophagy through reducing TNFSF11 expression and inhibiting PI3K/AKT/mTOR signaling in cartilage. Cell Mol Biol Lett 2022;27(1):62.
- [37] Young C, Kobayashi T. Limited roles of Piezo mechanosensing channels in articular cartilage development and osteoarthritis progression. Osteoarthritis Cartilage 2023;31(6):775–9.
- [38] Ma N, Zhang Z, Liao F, et al. The birth of artemisinin. Pharmacol Ther 2020;216:107658.
- [39] Talman AM, Clain J, Duval R, Ménard R, Ariey F. Artemisinin Bioactivity and Resistance in Malaria Parasites. Trends Parasitol 2019;35(12):953–63.